A seed-specific transcription factor, HSFA9, anticipates UV-B light responses by mimicking the activation of the UV-B receptor in tobacco

Raúl Carranco[†], Pilar Prieto-Dapena[†], Concepción Almoguera and Juan Jordano[*] (iD)

Instituto de Recursos Naturales y Agrobiología de Sevilla, Consejo Superior de Investigaciones Científicas (IRNAS-CSIC), Sevilla, Spain

*For correspondence (e-mail juan.jordano@csic.es)
[†]These authors contributed equally to this work.

SUMMARY

Sunflower heat shock factor A9 (HSFA9, hereafter A9) is a transcription factor involved in seed desiccation tolerance and longevity. A9 also links the regulation of seed maturation with that of seedling photomorphogenesis through visible light receptors. Analyses in transgenic *Nicotiana tabacum* (tobacco) indicated that A9 also affects responses mediated by NtUVR8, the receptor of ultraviolet light B (UV-B). We compared the effects of A9 and UV-B illumination on the nuclear localization of GFP-NtUVR8 in *Nicotiana benthamiana* leaves. We also used co-immunoprecipitation and limited proteolysis for analyzing the interaction between A9 and NtUVR8. We found that A9, by binding to NtUVR8, induced structural changes that resulted in enhancing the nuclear localization of NtUVR8 by hindering its nuclear export. The localization of UVR8 is crucial for receptor activation and function in Arabidopsis, where UV-B-activated nuclear UVR8 binds the E3 ubiquitin ligase COP1, leading to enhanced UV-B responses and photoprotection. A9 similarly activated NtUVR8 by enhancing COP1 binding without UV-B light. Seedlings and dark-germinated seeds that over-express A9 showed primed UV-B light stress protection. Our results unveil a UV-B-independent activation mechanism and a role for UVR8 in plant seeds that might contribute to early stress protection, facilitating seedling establishment.

Keywords: heat-shock transcription factor, *Helianthus annuus*, HSFA9, *Nicotiana tabacum*, Ultraviolet B light, UVR8 receptor, seed function, anticipated receptor activation.

INTRODUCTION

The integration of responses to light, temperature and other environmental cues with embryonic signaling promotes the acquisition of photosynthetic capacity after seed germination. This leads to a stage of plant development that is particularly sensitive to ambient stress. After germination, seeds transiently maintain their stress tolerance. The germinated seeds must quickly complete the development of the photosynthetic apparatus to ensure the survival of young seedlings after seed-stored reserves (proteins, lipids and carbohydrates) are exhausted. The synchronization and optimization of both processes are critical for ensuring efficient seedling establishment and high seedling vigor. The photosynthetic transition depends on light perception by different photoreceptors. Far-red and red lights are perceived, respectively, by the phytochrome A (PHYA) and B (PHYB) receptors (Chen & Chory, 2011; Christie et al., 2012; Franklin & Quail, 2010).

The blue and ultraviolet B (UV-B) light components of solar light are, respectively, perceived by cryptochromes (CRY) together with phototropins (PHOT), and by the UV RESISTANCE LOCUS 8 (UVR8) photoreceptor. All these photoreceptors facilitate the photosynthetic transition of emergent young seedlings. The diverse light receptors also contribute to enhancing tolerance to different kinds of environmental stress (Chaves et al., 2011; Christie, 2007; Christie et al., 2012; Rizzini et al., 2011).

Our lab has demonstrated the involvement of seed-specific transcription factors from the *HEAT SHOCK FACTOR* family (Guo et al., 2016; Scharf et al., 2012) in a regulatory link that operates between seed maturation and the photosynthetic transition after seedling emergence (Prieto-Dapena et al., 2017). In *Helianthus annuus* (sunflower) and similar crops, heat shock factor A9 (HSFA9) (hereafter A9; Almoguera et al., 2002) mainly activates this link (Almoguera et al., 2020). The A9 link involves, in part,

direct and indirect transcriptional effects on the PHYA and PHYB photoreceptor genes (Prieto-Dapena et al., 2017). A9 also enhanced responses to blue light mediated by the CRY1 receptor, in this case by increasing the accumulation of the CRY protein in seeds (Almoguera et al., 2020). A9, when overexpressed in transgenic tobacco plants, induced complex effects leading to accelerated photomorphogenesis (Prieto-Dapena et al., 2017). Such effects add to the enhanced tolerance to heat, drought and oxidative stress induced by A9 in seeds (Carranco et al., 2010; Prieto-Dapena et al., 2006, 2017) and in vegetative photosynthetic organs (see for example: Almoguera et al., 2012; Prieto-Dapena et al., 2008). We note that A9 in Asterid plants such as sunflower and *Nicotiana tabacum* (tobacco) might differ from HSFA9 in Arabidopsis, a Rosid dicot plant, as indicated by phylogenetic sequence analyses (see, Almoguera et al., 2002; Kotak et al., 2007). Transgenic tobacco is thus the heterologous system used in the previous publications of our lab to reproduce A9 function and regulation (see for example Carranco et al., 2010; Prieto-Dapena et al., 2006, 2017; Tejedor-Cano et al., 2010).

Transcriptomic analyses in transgenic tobacco indicated that A9 also affects responses mediated by UVR8, the UV-B light receptor, but not through direct effects on UVR8 transcript accumulation (Almoguera et al., 2020; see further details in Results). UVR8, originally discovered in the model plant Arabidopsis (Christie et al., 2012; Kliebenstein et al., 2002), has been found and partially characterized in other plants, including some crops (Dong et al., 2021; Fernández et al., 2020; Mao et al., 2015; Soriano et al., 2018; Tossi et al., 2019; Zhao et al., 2016). In Arabidopsis, UV-B is perceived by dimers of UVR8, which have a predominant cytosolic intracellular location. The UVR8 dimers monomerize following UV-B absorption and their nuclear localization is enhanced by changing the cytosolic–nuclear localization balance (Kaiserli & Jenkins, 2007). However, in some plants UVR8 is mostly monomeric before UV-B light perception (Soriano et al., 2018). In addition, Arabidopsis mutants with constitutively monomeric forms of UVR8 still respond to UV-B, e.g. UVR8$^{D96N, D107N}$, UVR8^{R286K} and UVR8^{G101S} (Heilmann et al., 2016; Podolec et al., 2021). The effects of UV-B on UVR8 involve structural changes that have been analyzed mainly for the Arabidopsis protein, for which 3D-conformation information is available (Camacho et al., 2019; Heilmann et al., 2015; Liao et al., 2019; Miyamori et al., 2015; Rizzini et al., 2011; Zeng et al., 2015). The UV-B-induced conformational changes allow nuclear-localized 'photo-activated' UVR8 to interact with the E3 ubiquitin ligase CONSTITUTIVELY PHOTOMORPHOGENIC 1 (COP1, Deng et al., 1991), thus promoting the stabilization and expression of transcription factors such as ELONGATED HYPOCOTYL 5 (HY5; Oyama et al., 1997; Ang et al., 1998), which, in turn, induce UV-B signaling (Favory et al., 2009; Lau et al., 2019;

Oravecz et al., 2006; Rizzini et al., 2011; Yin & Ulm, 2017). Studies in plants other than Arabidopsis suggest that these crucial post-transcriptional steps for UVR8 activation are mostly conserved (Reviewed by Tossi et al., 2019). We previously reported that A9 enhanced the nuclear localization of a second seed HSF, HSFA4a (A4a), leading to enhanced seed longevity and stress tolerance (Personat et al., 2014; Tejedor-Cano et al., 2010, 2014). This prompted us to investigate similar effects of A9 on UVR8. In this work we reveal novel link(s) between A9 and UVR8 and an underlying mechanism that is similar to what is known for the activation of UVR8 by UV-B in Arabidopsis. A9, through UVR8 and HY5, would trigger UV-B stress protection in the absence of acclimating UV-B illumination. This would be relevant for priming enhanced stress tolerance and photosynthetic transition immediately after seed germination, when very young seedlings emerge from the soil.

RESULTS

Hints of A9 effects on UVR8 signaling

To explore whether A9 regulates the expression and function of light receptors other than phytochromes (PHYA and PHYB; Prieto-Dapena et al., 2017) and cryptochromes (CRY1; Almoguera et al., 2020), we began by analyzing the published RNA-seq data for transcript accumulation changes induced by A9 in transgenic seeds and seedlings of tobacco (Almoguera et al., 2020). In particular, we analyzed the possible connection(s) between A9 and responses to UV-B light that are mediated by the UVR8 receptor. The A9 RNA-seq data indicate that the accumulation of transcripts for the predicted *N. tabacum* UVR8 protein (NtUVR8, XP_016473930), which is 99% identical to the proposed ancestral tobacco (*Nicotiana sylvestris* and *Nicotiana tomentosiformis*) UVR8 proteins (Fernandez et al., 2016), was not affected by A9. In contrast, RNA-seq data indicate that A9 enhanced the mRNA accumulation from genes that depend on both UVR8 and HY5, with HY5 a conserved transcription factor that functions as a hub for the convergent regulation of visible- and UV-light responses in plants (Gangappa & Botto, 2016). In Arabidopsis, over a thousand genes are directly activated by HY5, including most of the genes upregulated by UVR8 (see for example, Binkert et al., 2014; Brown et al., 2005; Brown & Jenkins, 2008; Favory et al., 2009; Oravecz et al., 2006). Among the 'target' genes of UVR8 and HY5 are four genes that are crucial for the synthesis of flavonoid 'sunscreen' photo-protectors: *chalcone isomerase* (*CHI*); *chalcone synthase* (*CHS*); *flavanone 3-hydroxylase* (*F3H*); and *flavonol synthase* (*FLS*). Also included is MYB12 that, like the similar transcription factors MYB13 (Qian et al., 2021) and MYB12-like, activates flavonol biosynthesis through CHI, CHS, F3H and FLS in a HY5- and UVR8-dependent pathway in tobacco and in other plants,

including Arabidopsis (reviewed by Yin & Ulm, 2017; see also Liu et al., 2020; Song et al., 2020). In experiments performed with imbibed seeds under darkness, we confirmed that A9, when expressed from the seed-specific DS10 promoter in the DS10:A9 lines (Prieto-Dapena et al., 2006), induced mRNA accumulation of CHI, CHS, F3H, FLS and MYB12 (Figure 1a). This was supported by observing converse effects with the loss of function of A9 in DS10:A9-SRDX seeds (Figure 1a; for the DS10:A9-SRDX lines, see Tejedor-Cano et al., 2010). Similar results were previously reported for HY5 transcripts (Prieto-Dapena et al., 2017). Together, the indications from our RNA-seq studies (Almoguera et al., 2020) and from the data in Figure 1(a) were consistent with the effects of A9 on NtUVR8, but not at the transcript level. We thus explored alternative mechanisms. In our experiments we used a GFP-NtUVR8 fusion protein, which, as shown in Figure 1(b), could be detected using either anti-GFP or anti-Arabidopsis UVR8 (C+ 426–440; Favory et al., 2009). This Arabidopsis UVR8 antibody detected protein(s) of the expected size (approx. 47.4 kDa) for NtUVR8 in tobacco seeds. Furthermore, the accumulation of the detected protein(s) (presumably NtUVR8) was enhanced by A9 (Figure 1c). Conversely (see also Figure 1c), the accumulation of the putative NtUVR8 protein(s) was impaired by the loss of function of A9 in DS10:A9-SRDX seeds. These results might be explained by direct/indirect transcriptional effects of A9 on genes involved in translation regulation. This inference is consistent with our published RNA-seq data. Thus, among the genes consistently upregulated by A9 we found at least 269 potentially involved in translation, including several ribosomal components and subunits of different translation initiation factors (Almoguera et al., 2020: figure 3; table S1).

A9 promotes the nuclear accumulation of NtUVR8

The results in Figure 2(a) show that UV-B illumination promoted the nuclear localization of GFP-NtUVR8. This UV-B response of GFP-NtUVR8 fits with the similar behavior of UVR8 in Arabidopsis (Kaiserli & Jenkins, 2007). Furthermore, when we used GFP fused to the Arabidopsis UVR8 protein, expressed and similarly treated with UV-B in our system, the nuclear relocalization effect was similar as with GFP-NtUVR8 (Figure S1). We could further confirm NtUVR8 as a functional UV-B receptor by complementing the *uvr8-1* mutation (Kliebenstein et al., 2002) in Arabidopsis using GFP-NtUVR8 (Figure S2). As A9 can induce the nuclear localization of transcription factors such as A4a (Tejedor-Cano et al., 2014), and because of the necessity of the nuclear localization of UVR8 for its function in Arabidopsis (for example, see Kaiserli & Jenkins, 2007), we studied whether A9 affects the nuclear localization of NtUVR8. As also shown in Figure 2(a), A9 enhanced the nuclear localization of GFP-NtUVR8 when both proteins were transiently co-expressed in *Nicotiana benthamiana*

leaves in the absence of UV-B illumination. Confocal microscopy under our experimental conditions showed similar, qualitative, nuclear localization of GFP-NtUVR8 only after treatment with either A9 or UV-B. In contrast, we note that A9 failed to induce the nuclear localization of GFP-AtUVR8 (Figure S1), which demonstrates the specificity of our assays and also reveals differences between AtUVR8 and NtUVR8. The A9-induced nuclear relocalization of GFP-NtUVR8 did not change the total accumulation level of the fusion protein (Figure S3); however, protein over-accumulation in our transient expression system might titrate post-transcriptional effects of A9, for example on the stability of the NtUVR8 protein. Direct or indirect interactions between A9 and NtUVR8 are likely behind the A9-induced relocalization. The interactions involving A9 might enhance the nuclear import of NtUVR8, or alternatively impair its nuclear export, or affect both processes. Nuclear export and import of GFP-NtUVR8 were broadly investigated in our system by, respectively, assessing the effects of leptomycin B (LMB), an inhibitor of nuclear exportins, and of sodium azide (NaN$_3$), which has been used to impair active nuclear transport (Twyffels et al., 2013). The results presented in Figure 2(a, bottom row) showed that treatments with LMB caused a similar nuclear relocalization of GFP-NtUVR8 as that observed with A9 or UV-B. Therefore, GFP-NtUVR8 is exported from the nucleus by a mechanism that involves exportins and nuclear export sequences (NESs). In addition, NaN$_3$ treatments impaired the UV-B-induced relocalization of GFP-NtUVR8. These results would support basal (non-dependent on A9 or UV-B), active nuclear import for GFP-NtUVR8 (Figure 2b).

We next explored which NtUVR8 sequences are potentially involved in the A9-induced relocalization of GFP-NtUVR8. For this purpose we analyzed the effect of a deletion of two conserved regions in UVR8, which in Arabidopsis have been shown to be involved in protein–protein interactions: the N-terminal and C-terminal parts of UVR8 (Figure 2a, ΔN30 and ΔC45). The previously reported UVR8 interactions include that with COP1 and others with different transcription factors and proteins, such as BES1, BIM1, DRM2, MYB13, MYB73/77, RUP1, RUP2 and WRKY16 (Cloix et al., 2012; Gruber et al., 2010; Qian et al., 2021; Yang et al., 2018, 2020; Yin et al., 2015). Some of these interactions are relevant for the nuclear localization of UVR8 (Cloix et al., 2012; Kaiserli & Jenkins, 2007; Qian et al., 2016; Yin et al., 2016). We also analyzed a three-amino-acid substitution in a potential NES sequence in NtUVR8 that is conserved in Arabidopsis UVR8 (Figure 2a, M3). The M3 substitutions were designed to inactivate the potential NES, in a similar way as previously reported for the A4a NES (Tejedor-Cano et al., 2014). We found that the deletions tested in NtUVR8 (ΔN30 or ΔC45), as well as the M3 mutant form of NtUVR8, did not relocate to the nucleus, either when induced by UV-B (in the absence of
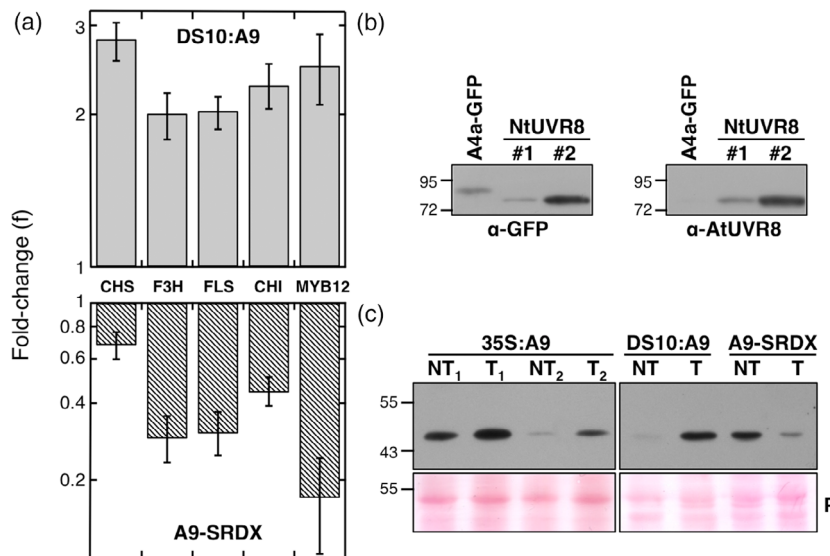
Figure 1. Indications for A9 effects on UVR8 signaling. (a) Top, RT-qPCR analyses for CHS, F3H, FLS, CHI and MYB12 transcript accumulation in DS10:A9 seeds. RT-qPCR fold-change (f) induced by A9 in transgenic (DS10:A9) compared with non-transgenic (NT) seeds, both of which were dark-imbibed for 24 h. Two different pairs of homozygous transgenic and NT sibling lines were analyzed in at least two experiments. Below, similar analyses for DS10:A9-SRDX seeds. Error bars denote SEs. (b) Western detection of the GFP-NtUVR8 fusion protein (NtUVR8) in agroinfiltrated leaves of *Nicotiana benthamiana*. Antibodies against GFP (α-GFP, left panel) or against Arabidopsis UVR8 (α-AtUVR8, right panel) were used with samples from two different experiments (#1 and #2). A different GFP-fusion protein, A4a-GFP (Tejedor-Cano et al., 2014), was included as a specificity control in both panels. (c) The Arabidopsis UVR8 antibody detects protein(s) of the expected size for NtUVR8 in *Nicotiana tabacum* (tobacco). The accumulation level of the NtUVR8 protein(s) detected was enhanced by A9 in seedlings germinated and kept under darkness for 10 days (35S:A9, left panel) and in seeds imbibed for 24 h without light (DS10:A9, right panel). Conversely, the accumulation of the putative NtUVR8 protein(s) was impaired by the loss of function of A9 (A9-SRDX, right panel). Samples from transgenic (T) and NT sibling lines were compared in both cases: two different pairs for 35S:A9 and single, representative, pairs for DS10:A9 and A9-SRDX. Ponceau S (P) staining was used as a control for protein loading (bottom panel). The position of molecular size markers (kDa) is depicted to the left of the panels in (b) and (c).

A9) or when co-expressed with A9 (in the absence of UV-B). Thus, the results summarized in Figure 2(a) strongly suggest that an intrinsic property of NtUVR8, e.g. its 3D conformation, is similarly affected by the UV-B treatment and by A9. The deleted NtUVR8 regions (in ΔN30 and ΔC45) and the mutated amino-acids (in M3) are required for the relocalization of GFP-NtUVR8, involving either A9 or UV-B. In particular, the results with the M3 mutant form suggest that the amino-acid substitutions tested affected the structural integrity of NtUVR8, rather than the *in silico* predicted (but not functionally confirmed) NES. From the results in Figure 2(a) we deduce that at least one NES is present elsewhere in the ΔN30 protein. The inferred NES is likely to be exposed in the structure of NtUVR8 before exposure to A9 or UV-B. Furthermore, A9 and UV-B would similarly affect the structure of NtUVR8 and hinder the exposed NES.

Our data also indicate that the effects of A9 on nuclear import of GFP-NtUVR8, if any, would be less relevant for the A9-induced relocalization. With regards to NtUVR8, we note that the required C45 amino acids may contribute to basal nuclear import. This is inferred from the failure of LMB to inhibit the relocalization of ΔC45 in contrast to what is observed for the ΔN30 and M3 fusion proteins (Figure 2a). Indeed, NLS sequences would be present in the

C45 NtUVR8 fragment, as C45 fused to GFP mainly localized in the nucleus, in contrast to the GFP control (Figure S4). The inferred NLS present in C45 would directly or indirectly (for example through bound COP1) mediate the nuclear import of NtUVR8. We also investigated possible effects of deletions and mutations in A9 on the A9-induced relocalization of GFP-NtUVR8, but all A9 variants tested functioned like wild-type (WT) A9. These variants included a tagged C-terminal deletion of A9 (A9ΔC), which we subsequently used for additional experiments (see below), and a nuclear localization sequence (NLS) mutant form of A9 (A9mNLS). The results with A9mNLS showed that the A9 NLS is not required for the relocalization of GFP-NtUVR8 (Figure 3). However, DsRed2-A9mNLS, which in contrast to DsRed2-A9 (Tejedor-Cano et al., 2014) is a nuclear-excluded protein (Figure S5), was still able to induce the nuclear localization of GFP-NtUVR8, perhaps through effects involving additional proteins (see the Discussion).

A9 interacts with NtUVR8

The main inference from the results summarized in Figure 2(a), that A9, through direct or indirect binding to NtUVR8, induces conformational changes similar to that caused by UV-B irradiation, was further supported with

Figure 2. UV-B and A9 (without UV-B) similarly promote the nuclear localization of GFP-NtUVR8. (a) GFP-NtUVR8 fusion protein (NtUVR8), deletion fusion proteins (ΔN30 and ΔC45) and the mutant (M3) used for the agroinfiltration experiments performed in leaves of *Nicotiana benthamiana*. In control conditions the localization of GFP-NtUVR8 was mostly cytosolic (Control). Treatment with UV-B or co-infiltration with HSFA9 (A9) increased the nuclear localization of GFP-NtUVR8. In contrast, all the deletion and mutant forms of NtUVR8 did not relocate to the nucleus when treated with UV-B (in the absence of A9) or when co-infiltrated with A9. Similarly, leptomycin B treatment (LMB) also enhanced the nuclear localization of GFP-NtUVR8. (b) Treatments with sodium azide (NaN₃) impaired the nuclear localization of the NtUVR8 fusion protein. For further details, see the Experimental procedures. Scale bars: 30 μm.
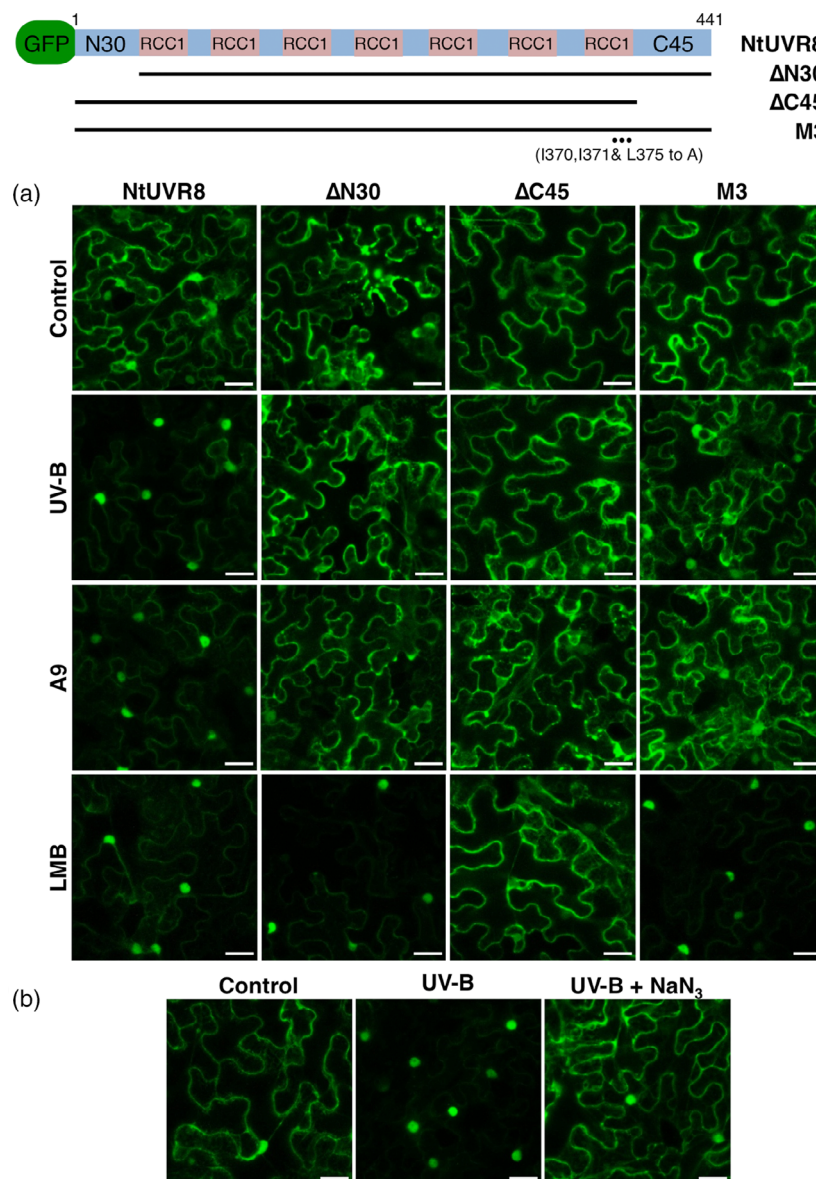
additional experiments. We first attempted to detect the expected interaction in yeast (*Sacharomyces cerevisiae*), using a two-hybrid approach that has worked for interactions between UVR8 and different proteins (see for example, Liang et al., 2018; Yang et al., 2018, 2020; Yin et al., 2015). As this approach failed (Figure S6), perhaps indicating the requirement of additional plant-specific protein(s) and(or) protein modification(s), we turned to *in planta* bimolecular fluorescence complementation (BiFC) and co-immunoprecipitation (CoIP). BiFC results were not conclusive because of the high background of non-specific interactions (data available upon request). However, CoIP clearly showed that A9 and NtUVR8 did indeed interact *in planta*, most likely helped by additional protein(s) (Figures 4 and S7). In the experiments of

Figure 4, and because of its higher solubility and accumulation level, we used A9ΔC instead of the full A9, as both forms caused similar relocalization effects on GFP-NtUVR8 (Figure 3). In addition, and because we expected a transient interaction, we introduced a formaldehyde cross-linking step in our CoIP protocol (see Experimental procedures). The interaction between NtUVR8 and A9ΔC was detectable without formaldehyde treatment (Figure S8), but the cross-linking step was used regularly, as it enhanced the detection and reproducibility of the observed interactions. Deletion of the oligomerization domain (OD) of A9 combined with the ΔC deletion did not affect the observed interaction (Figure S8). Thus, the A9 sequences required for interaction with NtUVR8 do not include the two regions that are relevant for protein–protein
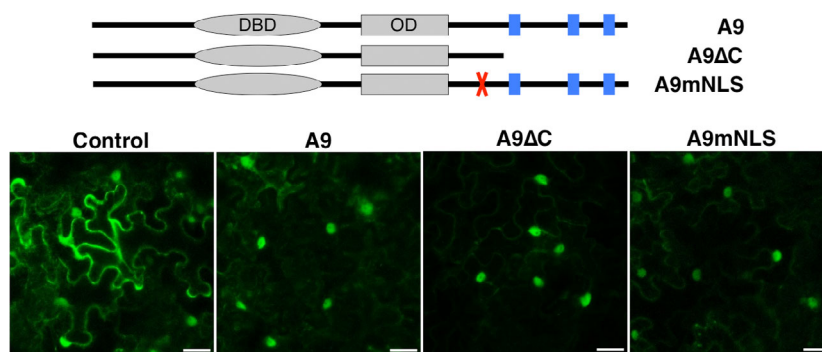
Figure 3. Deletions and mutations in A9 without effects on the A9-induced relocalization of GFP-NtUVR8. The wild-type (WT) A9 protein (A9) and mutant (A9ΔC and A9mNLS) forms depicted above were analyzed using GFP-NtUVR8 in agroinfiltration experiments performed in leaves of *Nicotiana benthamiana*, as described in Figure 2. Scale bars: 30 μm. The schematic indicates the position of the DNA binding (DBD) and oligomerization (OD) domains in A9. The C-terminal activation domain includes the AHA motifs, indicated with three small blue boxes. The position of the mutant nuclear localization sequence (NLS) in A9mNLS is indicated with a red cross.

interactions in previous reports for A9 and similar HSFs: the C-terminal region, which contains the transcriptional activation domain, and the OD (see for example, Carranco et al., 2010; Diaz-Martin et al., 2005; Scharf et al., 2012).

Strikingly, all the NtUVR8 deletion and mutant forms that we tested for the A9 effect on localization in Figure 2 (a) interacted with A9ΔC. In fact, and except for the ΔC45 form (Figure 4a), the observed interaction was similar as that with the complete GFP-NtUVR8 protein (Figure 4b). Using ΔC45 we observed an impaired interaction with A9ΔC (Figure 4a), but neither the C45 nor the N30 fragments by themselves interacted with A9ΔC (Figure 4c). We conclude that the C45 fragment of NtUVR8 is involved, but not sufficient, for *in planta* interaction with A9. The results obtained in Figure 4(b) for the ΔN30 and M3 fusion proteins are consistent with our interpretation of the data in Figure 2(a): that the ΔN30 and M3 regions of NtUVR8 would be involved in 3D-conformational changes induced by A9, rather than in binding A9.
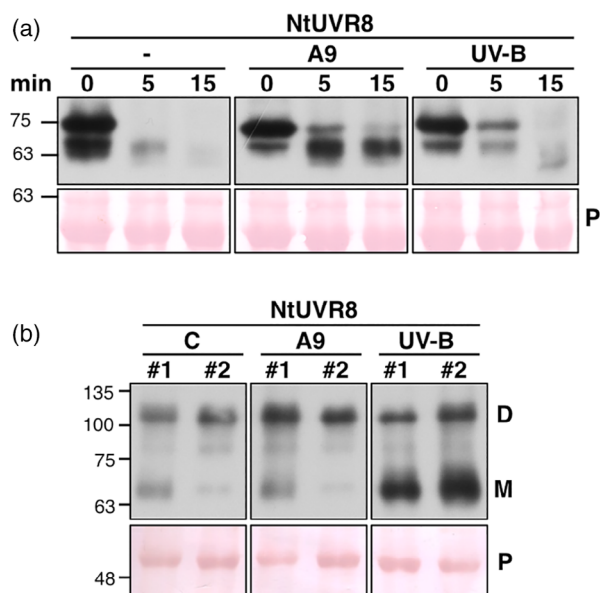
UV-B and A9 induce proteolytic protection of GFP-NtUVR8

To broadly assess conformational changes in NtUVR8, we performed limited proteolysis assays using trypsin A and extracts from leaves of *N. benthamiana* plants agroinfiltrated with GFP-NtUVR8. Control plants and the effects of UV-B illumination or A9 overexpression (under conditions as described in Figure 2a) were compared. The results in Figure 5(a) showed protection from proteolytic digestion, with respect to the control plants, in both experimental conditions: with the UV-B treatment (in absence of A9) and with transiently expressed A9 (in absence of UV-B illumination). These results support our inference from the results in Figure 2(a): the resemblance of conformational changes in NtUVR8 that are caused by A9 and UV-B. However, we should note that we used quite a crude assay of conformational change here, and there is some difference between
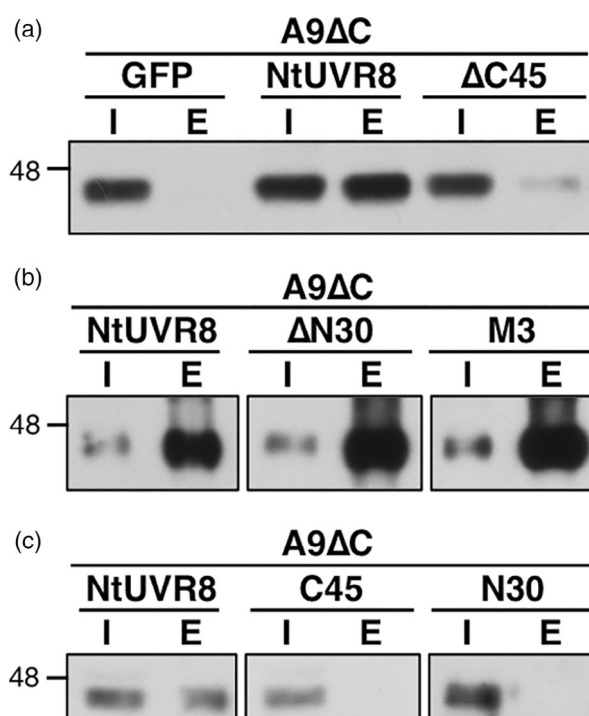
Figure 4. *In planta* interaction between A9 and different NtUVR8-GFP fusion proteins. Co-immunoprecipitation (CoIP) GFP-trap assays of HA-tagged A9ΔC using formaldehyde cross-linked samples from agroinfiltrated leaves of *Nicotiana benthamiana*: (a) interaction with the full-length NtUVR8 and the NtUVR8ΔC45 (ΔC45) fusion proteins; (b) interaction with the NtUVR8ΔN30 (ΔN30) and NtUVR8M3 (M3) fusion proteins; (c) fusions that only contain the N30 or C45 fragments of NtUVR8 did not interact with A9ΔC. In all cases we compared the input (I) to the eluted (E), bound, A9ΔC, which was detected using anti-HA. For further details, see Experimental procedures. The position of the molecular size markers (kDa) is given.

the results with A9 and UV-B in Figure 5(a,e,g) in the banding at 15 min. The deduced conformational changes caused by A9 in NtUVR8 are further supported by the results of protein–protein interaction in Figure 4(b). We

Figure 5. UV-B and A9 induce similar structural changes in NtUVR8. (a) Similar proteolytic protection of GFP-NtUVR8 (NtUVR8) in leaves of *Nicotiana benthamiana*. The GFP-NtUVR8 fusion protein was agroinfiltrated with or without A9, and the protein extracts were subjected to limited digestion with trypsin A from 0 to 15 min at 37°C. UV-B treatments (in the absence of A9) as described in Figure 2(a). (b) The dimeric (D) and monomeric (M) status of GFP-NtUVR8 was analyzed in agroinfiltrated leaves of *N. benthamiana*. The fusion protein was detected with anti-GFP, after SDS-PAGE (10%) using non-boiled Laemmli buffer extracts. Control conditions (C). Results shown for samples from two different experiments (#1 and #2). Ponceau S (P) staining was used as a control for overall protein accumulation level during trypsin A treatment (a) and loading (a, b). The position of molecular size markers (kDa) is given.

also note that GFP-NtUVR8 migrated in electrophoretic gels with a mobility consistent with being mostly dimeric, and that UV-B illumination, but not A9 co-expression, enhanced its monomerization (Figure 5b). Considering this differential effect, the conformational effects caused by A9 and UV-B on GFP-NtUVR8 would not be identical. Furthermore, it is likely that A9 binds the dimeric form of GFP-NtUVR8 inducing conformational changes that do not substantially alter its dimer/monomer status.

A9 (in the absence of UV-B) enhances the binding of Arabidopsis COP1 to NtUVR8

The results reported so far indicate that A9 might activate NtUVR8 in the absence of UV-B. This would have functional relevance, for example, in germinated seeds before their emergence from the soil. The deduced resemblance between the structural effects of UV-B and A9 on GFP-NtUVR8 (Figures 2a and 5a) also suggest a possible mechanism: that A9, as UV-B in Arabidopsis and other plants, might facilitate the binding of COP1 to UVR8 (Cloix et al., 2012; Favory et al., 2009; Rizzini et al., 2011). We analyzed this suggestion by performing CoIP experiments in leaves of *N. benthamiana* using the same system as

described in Figure 4. In these experiments we used Arabidopsis COP1, as it was previously shown to interact with *Solanum lycopersicum* (tomato) UVR8 (Dong et al., 2021), and because putative COP1 orthologs in *N. tabacum* are not yet confirmed. In addition, the A9ΔC protein was used, as it is a HA-tagged protein suitable for CoIP that interacted with GFP-NtUVR8 and enhanced its nuclear localization in a similar way as the complete A9 protein (see Figures 3, 4 and S7). In our system (see Figures 6a and S7), unfused GFP (when co-expressed with COP1) did not interact with COP1. In contrast, there was a basal – but marginal – interaction between COP1 and GFP-NtUVR8 that was drastically enhanced by UV-B illumination (in the absence of A9ΔC). When A9ΔC, GFP-NtUVR8 and COP1 were co-expressed,
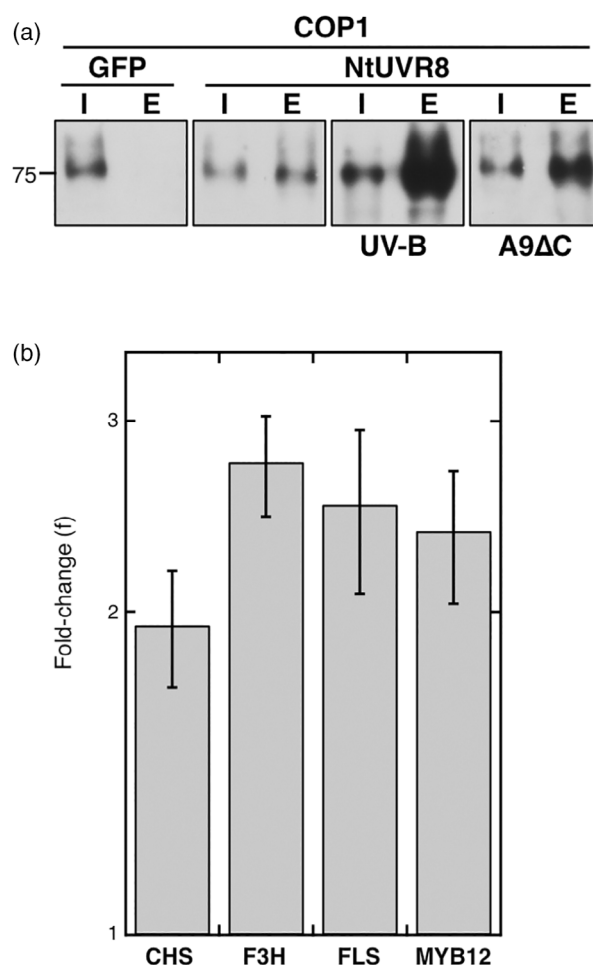

Figure 6. A9 enhances the binding of COP1 to NtUVR8. Co-immunoprecipitation (CoIP) GFP-trap assays of HA-tagged *Arabidopsis thaliana* COP1 (COP1) with GFP (GFP) or GFP-NtUVR8 (NtUVR8). (a) The NtUVR8 samples were analyzed, essentially as described in Figure 4, without or with UV-B treatment, as described in Figure 2(a) (UV-B), or with co-expressed A9ΔC (A9ΔC). The position of molecular size markers (kDa) is given. The detected basal binding of COP1 to NtUVR8 was enhanced by either UV-B or A9ΔC. (b) In dark-germinated seeds, A9ΔC induced the accumulation of CHS, F3H, FLS and MYB12 transcripts in a similar way as was observed with A9 in Figure 1(a).

the binding of COP1 to GFP-NtUVR8 was also enhanced, this time in the absence of UV-B illumination. This result prompted us to study possible effects of A9ΔC on the endogenous NtUVR8 using stably transformed DS10:A9ΔC lines. The results in Figure 6(b) showed that, in dark-germinated seeds, A9ΔC induced the accumulation of CHS, F3H, FLS and MYB12 transcripts in a similar way as observed with the complete A9 protein in the DS10:A9 lines (see also Figure 1a). As the transcription of CHS, F3H, FLS and MYB12 depends on UVR8 via HY5 (reviewed by Yin & Ulm, 2017; Binkert et al., 2014; Liu et al., 2020) our results are consistent with A9ΔC indirectly affecting HY5 as a result of the enhanced binding of endogenous COP1 to NtUVR8 in the absence of UV-B illumination. The results in Figure 6 support the hypothesis that A9 would 'activate' NtUVR8 without UV-B in a similar way as UV-B activates

UVR8 in Arabidopsis, leading to enhanced binding and the sequestration of COP1 (Lau et al., 2019).

A9 enhances UV-B stress protection in transgenic tobacco

We used A9 transgenic lines to confirm the UV-B stress protection expected from the effects of A9 on NtUVR8 and COP1 described so far. We could not analyze other possible effects, such as UV-B-induced photomorphogenesis, perhaps because of interference caused by the functional interaction of A9 with additional receptors (Almoguera et al., 2020), in particular with blue-light receptors such as CRY1 (Rai et al., 2019). We could clearly observe primed protection from UV-B damage using non-acclimated transgenic seedlings that ectopically overexpress A9 (35S:A9; Prieto-Dapena et al., 2008; Figure 7a). The quantification of total chlorophyll and carotenoid pigments 8 days after the
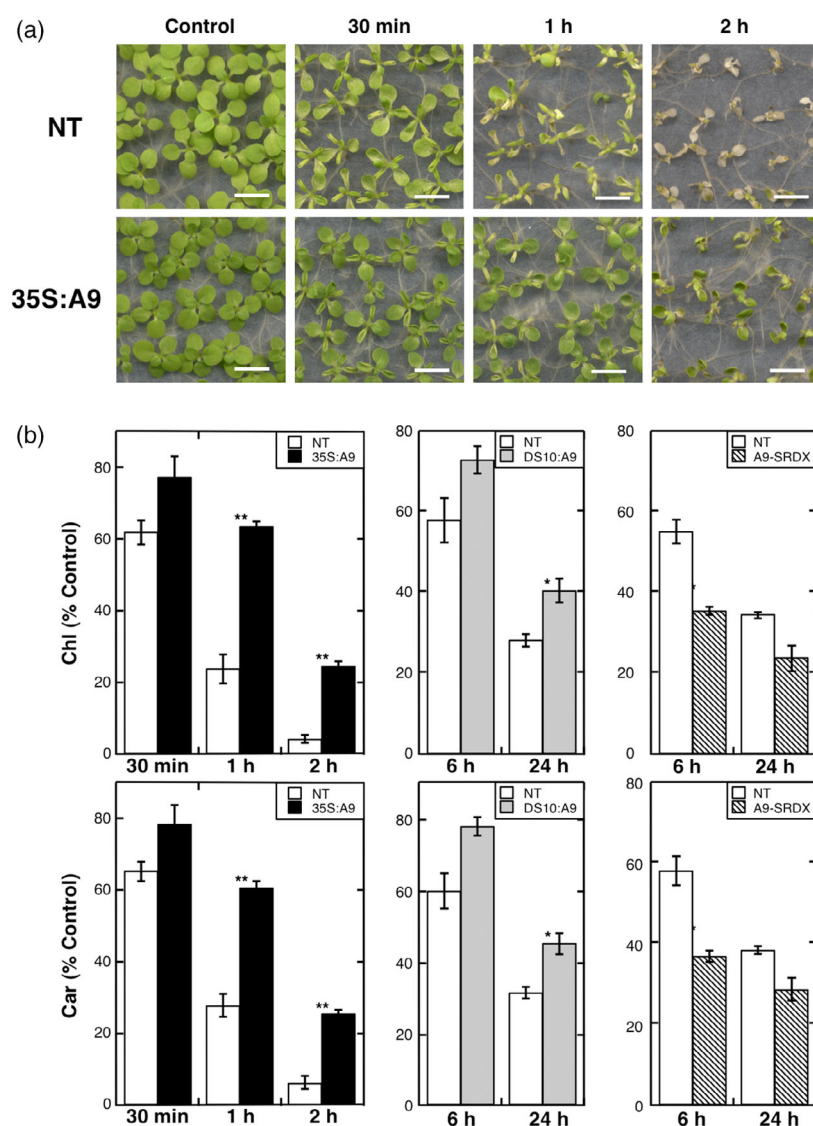
Figure 7. A9 enhances UV-B photoprotection in transgenic tobacco. (a) Non-acclimated 35S:A9 seedlings that constitutively overexpress A9 resisted UV-B stress conditions that damaged non-transgenic (NT) siblings. Three-week-old seedlings were treated with broadband UV-B from 30 min to 2 h (as indicated), or without UV-B (Control). Representative results are shown with pictures taken after stress recovery. Scale bars: 7 mm. (b) Quantification of total chlorophyll (top) and carotenoids (bottom) 8 days after UV-B treatment of 35S:A9 seedlings, DS10:A9 seeds and DS10:A9-SRDX (A9-SRDX) seeds (see the Experimental procedures). Average values, shown as percentages with respect to control values, are depicted for experiments performed with two pairs of sibling NT and transgenic lines (35S:A9 or DS10:A9). Error bars denote the SEs. Asterisks denote statistically significant differences (*$P < 0.05$, **$P < 0.01$).

damaging UV-B treatments showed that the 35S:A9 seedlings resisted the treatments much better than non-transgenic, sibling, seedlings (Figure 7b). Similar quantitative analysis and observations were obtained using imbibed seeds from transgenic lines that seed-specifically overexpress A9 (DS10:A9; Prieto-Dapena et al., 2006). Furthermore, converse effects were observed upon the loss of function of A9 in DS10:A9-SRDX seeds (see also Figure 7b). This confirmed the A9-primed UV-B stress protection in a native (seed) context (Figure 7b). The observed protection is consistent with the different effects of A9 on UVR8 reported here (Figures 1–6). These effects, and the previously reported effects of A9 on HY5 and different photoreceptors (Almoguera et al., 2020; Prieto-Dapena et al., 2017), would contribute to the observed UV-B photoprotection.

DISCUSSION

Plants respond and adapt to sunlight UV-B through signaling initiated by the UVR8 receptor. A molecular mechanism for the UVR8-mediated response is still incomplete, but it has been outlined from studies mostly carried out in Arabidopsis. Crucial steps in the UVR8-mediated response have been confirmed in species from green algae, such as *Chlamydomonas* spp., to higher plants, including dicots (Tossi et al., 2019; Yin & Ulm, 2017). In sum, UV-B disrupts UVR8 dimers that are predominantly located in the cytosol. UV-B-induced conformational changes in UVR8 also promote its nuclear localization and affect conserved sequences in the C-terminal region of UVR8 that interact with COP1 (Cloix et al., 2012; Kaiserli & Jenkins, 2007; Qian et al., 2016; Yin et al., 2016). The UV-B-induced interaction of UVR8 with COP1, in turn, results in the stabilization of HY5; subsequent molecular effects lead to enhanced photoprotection and photomorphogenic effects, such as the suppression of hypocotyl extension in seedlings (Favory et al., 2009; Lau et al., 2019; Rizzini et al., 2011). Our results suggest a similar mechanism for the A9-induced activation of NtUVR8 in tobacco plants in the absence of UV-B illumination. A9 binds NtUVR8 sequences including the C-terminal and the C45 fragment that harbors a conserved C27 sequence with VP amino-acid motifs, which has been shown to be the target of different protein–protein interactions that depend (COP1, MYB73/75 and MYB13) or not (WRKY36, BIM1, BES1 and DRM2) on UV-B (Cloix et al., 2012; Jiang et al., 2021; Liang et al., 2018; Qian et al., 2021; Yang et al., 2018, 2020). The A9–NtUVR8 interaction reported here does not require UV-B. Our *in planta* analyses of the A9-induced nuclear localization (Figure 2), of the A9–NtUVR8 protein interaction (Figure 4) and of limited proteolysis (Figure 5a) all support the hypothesis that in the absence of UV-B illumination, the binding of A9 induces conformational changes in NtUVR8 that result in its proteolytic protection

and in hindering an exposed NES in NtUVR8; these A9-induced conformational changes lead to the promotion of nuclear accumulation of NtUVR8. A9 and UV-B would similarly affect the structure of NtUVR8 and hinder the exposed NES (Figures 2 and 5a). The 3D conformation of UVR8 has been analyzed only in Arabidopsis and in connection with the perception of UV-B (Camacho et al., 2019; Heilmann et al., 2015; Liao et al., 2019; Miyamori et al., 2015; Rizzini et al., 2011; Zeng et al., 2015). Briefly, in response to UV-B the structure of UVR8 is subtly altered by conformational changes that involve different regions of the receptor protein: the β-propeller core and the N-terminal and C-terminal extensions, with the C-terminal extension including conserved C27 sequences that, as noted above, are targeted by different protein–protein interactions, including COP1. We propose that the C-terminal fragment of NtUVR8 (C45), also an N-terminal N30 fragment, and the conserved I370, I371 and L373 amino acids changed in the M3 mutant of NtUVR8 participate in the UV-B-induced and A9-induced conformational changes, both of which lead to the enhanced binding of COP1, as observed in the UV-B-induced response in Arabidopsis (Cloix et al., 2012; Yin et al., 2015), as deduced from the results in Figures 2, 5(a) and 6(a). However, UV-B illumination enhanced GFP-NtUVR8 monomerization, in contrast to what is observed with A9 (Figure 5b). This suggests that in NtUVR8, monomerization and receptor activation are not intrinsically linked, at least in response to A9 in the absence of UV-B. Furthermore, the results of Figures 3 (A9mNLS data) and 5(b) support that A9 binds the dimeric form of NtUVR8, and that this binding might occur both before and after NtUVR8 is imported to the nucleus. Regarding the UV-B responses in Arabidopsis we note that monomerization and receptor activation could also be uncoupled, but only using different constitutively monomeric mutant forms of UVR8, such as UVR8$^{D96N, D107N}$, UVR8^{R286K} and UVR8^{G101S} (Heilmann et al., 2016; Podolec et al., 2021). Thus, the proposed activation mechanism of NtUVR8 by A9 would differ from the UV-B-induced activation in that the A9-induced conformational changes do not lead to substantial receptor monomerization. However, both activation mechanisms would involve similar but not identical conformational changes, leading to enhanced binding and the sequestration of COP1, as demonstrated in Arabidopsis for UVR8 in connection with the UV-B response (Lau et al., 2019). The UV-B-induced sequestration of COP1 in turn impairs the degradation of the HY5 protein, subsequently enhancing HY5-dependent transcription by a mechanism beyond HY5 transcriptional regulation (Favory et al., 2009; Lau et al., 2019; Rizzini et al., 2011). We should note that our results indicate that in the presence of A9, COP1 presumably binds to dimeric UVR8, which supports the hypothesis that conformational change rather than monomer formation *per se* may

promote COP1 binding in UV-B. By binding dimeric NtUVR8 in the cytosol the NLS mutant form of A9 (A9mNLS), like the WT A9, would also induce persistent conformational change(s) that 'dark-activate' NtUVR8 and prevent its nuclear export (see Figure 3). Persistent change(s) might also facilitate NtUVR8 nuclear import, which does not require the NLS of A9, but perhaps it is helped by protein(s), such as COP1, bound to 'dark-activated' NtUVR8 that might 'lock' the A9- induced conformational change(s).

A9 is a seed-specific transcription factor that disappears shortly after seed imbibition (Almoguera et al., 2002). NtHSFA9 and NtUVR8 coexist in tobacco seeds after germination and before seedlings emerge from the soil. In that context, A9 and ortholog HSFA9 transcription factors, including NtHSFA9, might prime early UV-B responses and stress tolerance in germinating seeds. Here, we could show that A9 indeed primed resistance to UV-B stress when ectopically, or seed-specifically, overexpressed in transgenic tobacco, with results that were confirmed with loss-of-function lines (Figure 7b). In sum, through transcriptional effects on HY5 (Prieto-Dapena et al., 2017) and different post-transcriptional effects that enhance the accumulation (Figure 1c) and activity of the NtUVR8 receptor (Figure 6), A9 pre-conditioned the seeds for stress tolerance without previous exposure to UV-B irradiation in a similar way as is described for UV-B priming in seeds (Bera et al., 2021; Thomas & Puthur, 2017). Our proposed activation mechanism for NtUVR8, and the additional effects of A9 on NtUVR8 reported here, would unveil and support a novel, UV-B-independent, role for UVR8 in seeds.

EXPERIMENTAL PROCEDURES

Plant material

The sibling pairs of non-transgenic and transgenic tobacco lines used in this report were obtained after segregation and propagation from single-integration homozygous lines, described in our earlier publications (DS10:A9, Prieto-Dapena et al., 2006; 35S:A9, Prieto-Dapena et al., 2008; DS10:A9ΔC and DS10:A9-SRDX, respectively M1 and M3 in Tejedor-Cano et al., 2010). Each transgene was integrated at different genomic locations. Seed sterilization, germination, and seedling growth under controlled photoperiodic conditions of 16-h light/8-h dark were performed as described previously (Prieto-Dapena et al., 2017).

In planta expression and protein localization assays

These experiments were performed basically as described by Tejedor-Cano et al. (2014). *Nicotiana benthamiana* plant leaves (4 weeks old) were infiltrated with mixtures of *Agrobacterium* strains that contained the required plasmid combinations. After infiltration, plants were placed back in the growing chamber and, after 48 h, disc sections of the infiltrated leaves were analyzed with a confocal laser-scanning microscope (FV1000; Olympus, https://www.olympus-global.com), using an UPLSAPO 60×W NA:1.20 objective and standard GFP or DsRed filter settings (Tejedor-Cano et al., 2014). Image analysis was performed with

FV10-ASW 1.7. Image acquisition conditions were adjusted for each sample, to avoid signal saturation.

The hemagglutinin (HA)-tagged HA-A9 (A9) and HA-A9ΔC (A9ΔC) were expressed from plasmids pBI121-HA-HaHSFA9 and pBI121-HA-HaHSFA9 M1, respectively (Tejedor-Cano et al., 2010). DsRed2-A9mNLS (A9mNLS) was expressed from pRCS2-nptII-DsRed::A9mNLS. This plasmid was made from pRCS2-nptII-DsRed::A9 (Tejedor-Cano et al., 2014) using the Q5® Site-Directed Mutagenesis kit (New England BioLabs, https://international.neb.com) with the oligonucleotide A9mutNLS forward primer and the mutant oligonucleotide A9mutNLS reverse primer (all primers are described in Table S1). A9Δ(OD+C) was expressed from pBI121-HA-A9Δ(OD+C). This plasmid was made from pBI121-HA-HaHSFA9 M1 using the Q5® Site-Directed Mutagenesis kit and primers A9delOD.

GFP-NtUVR8 (NtUVR8) was expressed from plasmid pRCS2-nptII-GFP-UVR8. The GFP-NtUVR8 cassette, from pSAT-EGFP-UVR8, was introduced into pRCS2-nptII (Tejedor-Cano et al., 2014) at the PiPspI restriction site. To make pSAT-EGFP-UVR8, the NtUVR8 coding sequence (CDS) was obtained by PCR amplification of the 35S:A9 cDNA library (Almoguera et al., 2020), with primers UVR8 CDS1 (forward and reverse, see Table S1) and inserted in the pSPARK vector (Canvax Biotech, https://lifescience.canvaxbiotech.com). NtUVR8 CDS was recovered by PCR amplification with primers UVR8 CDS2 (forward and reverse, see Table S1). This amplicon, digested with BamHI, was inserted into SmaI- and BamHI-digested pSAT6-EGFP (Tejedor-Cano et al., 2014). GFP alone (GFP) was expressed as a control from plasmid pSAT6-EGFP. GFP-UVR8mutNES (M3) was expressed from plasmid pRCS2-nptII-GFP-UVR8mutNES. The GFP-UVR8mutNES cassette, from pSAT-EGFP-UVR8mutNES, was inserted into pRCS2-nptII binary vector using the PiPspI restriction site. pSAT-EGFP-UVR8mutNES was performed by PCR amplification of pSAT-EGFP-UVR8 with the UVR8mNES forward primer and the mutagenic oligonucleotide UVR8mNES reverse primer. The purified PCR product was used as a mega-primer for a second round of PCR amplification with the primer M13reverse. The final PCR product was digested with SphI and NotI to replace the corresponding WT fragment in pSAT-EGFP-UVR8. This resulted in three amino acid substitutions (to alanine) at positions I 374, I 378 and L 381. GFP-UVR8ΔN30 (ΔN30) was expressed from plasmid pRCS2-nptII-GFP-UVR8ΔN30. The GFP-UVR8ΔN30 cassette, from pSAT-EGFP-UVR8ΔN30, was introduced into pRCS2-nptII binary vector using the PiPspI restriction site. pSAT-EGFP-UVR8ΔN30 was performed by PCR amplification of pSAT-EGFP-UVR8 plasmid with the UVR8delN30 forward primer and the UVR8delN30 reverse fusion primer. The PCR product was digested with ApaI and SphI to substitute the corresponding fragment in pSAT-EGFP-UVR8. GFP-UVR8ΔC45 (ΔC45) was expressed from pRCS2-nptII-GFP-UVR8ΔC45. This plasmid was made from pRCS2-nptII-GFP-UVR8 using the Q5® Site-Directed Mutagenesis kit and the primer UVR8delC45. GFP-UVR8N30 (N30) was expressed from pRCS2-nptII-GFP-UVR8N30. This plasmid was made from pRCS2-nptII-GFP-UVR8 using the Q5® Site-Directed Mutagenesis kit and the primers UVR8 N30 (forward and reverse, see Table S1). GFP-UVR8C45 (C45) was expressed from pRCS2-nptII-GFP-UVR8C45. This plasmid was made from pRCS2-nptII-GFP-UVR8 using the Q5® Site-Directed Mutagenesis kit and primers UVR8 C45 (forward and reverse, see Table S1).

The AtCOP1 CDS (COP1) was expressed from pBI121::HA-AtCOP1. To make this plasmid, pBI121-HA-HaHSFA9 M1 was digested with SmaI and SalI and the released fragment was replaced by the HA-AtCOP1 cassette obtained from SmaI- and SalI-digested SK-HA-AtCOP1 plasmid. For SK-HA-AtCOP1 construction,

pGADT7 GW-AtCOP1 (Yin et al., 2015) was PCR- amplified with COP1 primers. The amplicon, digested with *Sal*I, was introduced in *Eco*RV- and *Sal*I-digested pB SK-3xHA. pB SK-3xHA was made by PCR amplification of pUC19-35S:HA:M1 (Tejedor-Cano et al., 2010) with PUC-HA primers, and the amplicon inserted in the *Eco*RV site of pBluescript SK.

Treatments of infiltrated leaves

For UV-B treatment, leaves harvested 48 h after infiltration were exposed to dim white light (3 μmol m^{-2} s^{-1}) supplemented with narrow-band UV-B (2 μmol m^{-2} sec^{-1}; TL 40W/01 UV-B lamp; Philips, https://www.philips.com) for 4 h. For sodium azide (NaN$_3$) treatment, 48 h after infiltration leaf discs were placed in 50 mM D-glucose solution and subjected to UV-B treatment. After 1 h, NaN$_3$ was added to reach 5 mM and samples were observed 2 h later. For LMB treatment, leaf discs were cut 24 h after infiltration and soaked with 100 nM LMB in 0.01% Tween-20 for 24 h in the growing chamber.

Co-immunoprecipitation assays

The proteins of interest were transiently expressed in *N. benthamiana* leaves, as indicated. Infiltrated leaves were harvested and proteins cross-linked in 400 mM sucrose, 10 mM Tris-HCl, pH 8.0, 5 mM β-mercapto-ethanol, 0.1 mM phenylmethylsulfonyl fluoride (PMSF) with 0.5% formaldehyde (or the indicated amount) for 15 min under vacuum at 24°C. The reaction was stopped with glycine (final 125 mM). Leaves were frozen and ground in liquid nitrogen. Proteins were extracted with five volumes of buffer IP (10 mM Tris-HCl, pH 8, 200 mM NaCl, 5% glycerol, 1% Triton X-100, 0.1 mM PMSF, 1 × Complete Protease Inhibitor Cocktail; Roche, https://www.roche.com) for 45 min at 4°C under rotation, with cellular debris removed by centrifugation (5 min at 12 000 ***g*** and 4°C). A 1400-μl volume of extract was incubated with 20 μl of ChromoTek GFP-Trap® Agarose beads for 2.5 h at 4°C under rotation. Beads were recovered by centrifugation (1 min at 500 ***g*** and 4°C) and washed three times in buffer IP. Unbound proteins were recovered (NB). Co-immunoprecipitated proteins (E) were obtained by heating for 5 min at 95°C in 2× Laemmli buffer. As an input control (I), 60 μl of protein extract was incubated with 60 μl of 2× Laemmli buffer and heated for 5 min at 95°C. A 4-μl volume of I (1.5 μl in Figures 4b and S7) and 10-μl volume of E were analyzed by Western blot. Proteins were detected with anti-HA-peroxidase antibody (Roche) at 1/1000 dilution for HA-tagged proteins or anti-GFP antibody (Abcam, https://www.abcam.com) at 1/8000 dilution for GFP-fusion proteins. Anti-rabbit IgG-peroxidase (GE Healthcare, https://www.gehealthcare.com) at 1/25 000 dilution was used as a secondary antibody for Western blots with anti-GFP.

Limited proteolysis assays

The proteins of interest were transiently expressed in *N. benthamiana* leaves, as indicated. Infiltrated leaves were frozen and ground in liquid nitrogen. Proteins were extracted with three volumes of extraction buffer (50 mM Tris-HCl, pH 7.5, 150 mM NaCl, 5 mM MgCl$_2$, 10% glycerol, 0.1% Nonidet P-40) for 60 min at 4°C under rotation, and cellular debris was removed by centrifugation for 10 min at 16 000 ***g***. A 500-μg portion of protein was made up to a volume of 150 μl with extraction buffer, with 1 μg of trypsin A added. Digestion was performed at 37°C and 15-μl aliquots were taken at different times (indicated in the legends), mixed with 5 μl of 4× Laemmli buffer and heated for 5 min at 65°C. Proteins were detected by Western blot with anti-GFP antibody, as indicated before.

UVR8 dimer analysis

Proteins were expressed and extracted as described for the limited proteolysis assays, but the extraction buffer was supplemented with 1 mM PMSF, 1 mM DTT, 1 mM Pefabloc SC (4-(2-aminoethyl) benzenesulfonyl fluoride hydrochloride, AEBSF) (Roche), and 1 × Complete Protease Inhibitor Cocktail (Roche). A 0.1-μl volume of proteins were diluted in 20 μL of 1× Laemmli buffer and loaded onto SDS-PAGE gels without heating. Western blots with anti-GFP antibody were performed as indicated for the limited proteolysis assays.

Real-time quantitative PCR

The RT-qPCR was performed as described by Prieto-Dapena et al. (2017). Total RNA was isolated from whole imbibed seeds with the LiCl method. The cDNA was prepared using the Maxima First Strand cDNA Synthesis Kit (ThermoFisher Scientific, https://www.thermofisher.com). RT-qPCR was performed using the SensiFastTM SYBR® No-ROX Kit (Bioline, https://www.bioline.com) in a Roche LightCycler 480 using standard PCR conditions, according to the manufacturer's instructions. Parallel reactions were used to normalize the quantity of template cDNA. Primers for transcript abundance normalization (*Ntubc2*, *L25* and *EF-1α*) are described by Prieto-Dapena et al. (2017). Primers for *CHI*, *CHS*, *F3H*, *FLS* and *MYB12* amplification are listed in Table S1. The reproducibility of RT-qPCR was achieved by running technical duplicates, and by using two independent cDNA preparations. At least two biological replicates were performed per set of conditions.

UV-B treatments of transgenic plants and chlorophyll and carotenoid quantification

Two different pairs of transgenic and non-transgenic (NT) lines were analyzed for UV-B stress resistance. Three-week-old 35S:A9 seedlings were treated with cellulose-acetate-filtered broadband UV-B (using Philips TL 40W/12 RS SLV/25 lamps) at 8 μmol m^{-2} s^{-1}, for 30 min to 2 h. Untreated seedlings were used as negative control. After UV-B stress, seedlings were allowed to recover in the growth chamber for 1 week. After recovery, pictures were taken and plant material was harvested for chlorophyll and carotenoid quantification, as described by Prieto-Dapena et al. (2017). For DS10:A9 and DS10:A9-SRDX transgenic lines, dark-germinated, 3-day-imbibed seeds were treated with broadband UV-B (as described for the 35S:A9 seedlings) for 6 or 24 h. Seed material was harvested for chlorophyll and carotenoid quantification after recovery for 1 week.

AUTHOR CONTRIBUTIONS

RC, PPD, CA and JJ designed the research. RC and PPD performed crucial experiments, including the cellular localization analyses, protein–protein interaction analyses and limited proteolysis. CA performed the experiments of NtUVR8 protein accumulation and UV-B stress protection. All authors analyzed the data and contributed to the additional experiments included as supporting information. JJ supervised the research and, with input from the other authors, wrote the article.

CONFLICT OF INTEREST

The authors declare that they have no conflicts of interest associated with this work.

DATA AVAILABILITY STATEMENT

The data that support the findings of this study are available from the corresponding author, upon request.

SUPPORTING INFORMATION

Additional Supporting Information may be found in the online version of this article.

Figure S1. Nuclear relocalization of GFP-AtUVR8 after UV-B illumination, but not with A9, under the experimental conditions of Figure 2.

Figure S2. Functional complementation of the *uvr8-1* mutant in Arabidopsis using GFP-NtUVR8.

Figure S3. Western detection of the accumulation of the GFP-NtUVR8 fusion protein (NtUVR8) in agroinfiltrated leaves of *Nicotiana benthamiana*.

Figure S4. The C45 of NtUVR8 fused to GFP (C45) showed predominantly nuclear localization.

Figure S5. The NLS mutation of A9 promotes nuclear exclusion.

Figure S6. Y2H interaction assays.

Figure S7. GFP-trap CoIP controls.

Figure S8. Effect of formaldehyde cross-linking on the interaction between A9 and GFP-NtUVR8.

Table S1. List of primers.

Data S1. Methods for UVR8 complementation in Arabidopsis and yeast two-hybrid.

REFERENCES

Almoguera, C., Prieto-Dapena, P., Carranco, R., Ruiz, J.L. & Jordano, J. (2020) Heat stress factors expressed during seed maturation differentially regulate seed longevity and seedling greening. *Plants*, **9**, 335. https://doi.org/10.3390/plants9030335

Almoguera, C., Prieto-Dapena, P., Personat, J.M., Tejedor-Cano, J., Lindahl, M., Diaz-Espejo, A. et al. (2012) Protection of the photosynthetic apparatus from extreme dehydration and oxidative stress in seedlings of transgenic tobacco. *PLoS One*, **7**, e51443. https://doi.org/10.1371/journal.pone.0051443

Almoguera, C., Rojas, A., Díaz-Martín, J., Prieto-Dapena, P., Carranco, R. & Jordano, J. (2002) A seed-specific heat-shock transcription factor involved in developmental regulation during embryogenesis in sunflower. *The Journal of Biological Chemistry*, **277**, 43866–43872. https://doi.org/10.1074/jbc.M207330200

Ang, L.H., Chattopadhyay, S., Wei, N., Oyama, T., Okada, K., Batschauer, A. et al. (1998) Molecular interaction between COP1 and HY5 defines a regulatory switch for light control of Arabidopsis development. *Molecular Cell*, **1**, 213–222. https://doi.org/10.1016/S1097-2765(00)80022-2

Bera, K., Dutta, P. & Sadhukhan, S. (2021) Seed priming with non-ionizing physical agents: plant responses and underlying physiological mechanisms. *Plant Cell Reports*, **1**, 1–21. https://doi.org/10.1007/s00299-021-02798-y

Binkert, M., Kozma-Bognár, L., Terecskei, K., De Veylder, L., Nagy, F. & Ulm, R. (2014) UV-B-Responsive association of the Arabidopsis bZIP transcription factor ELONGATED HYPOCOTYL5 with target genes, including its own promoter. *Plant Cell*, **26**, 4200–4213. https://doi.org/10.1105/tpc.114.130716

Brown, B.A., Cloix, C., Jiang, G.H., Kaiserli, E., Herzyk, P., Kliebenstein, D.J. et al. (2005) A UV-B-specific signaling component orchestrates plant UV protection. *Proceedings of the National Academy of Sciences of the United States of America*, **102**, 18225–18230. https://doi.org/10.1073/pnas.0507187102

Brown, B.A. & Jenkins, G.I. (2008) UV-B signaling pathways with different fluence-rate response profiles are distinguished in mature Arabidopsis leaf tissue by requirement for UVR8, HY5, and HYH. *Plant Physiology*, **146**, 576–588. https://doi.org/10.1104/pp.107.108456

Camacho, I.S., Theisen, A., Johannissen, L.O., Diaz-Ramos, L.A., Christie, J.M., Jenkins, G.I. et al. (2019) Native mass spectrometry reveals the conformational diversity of the UVR8 photoreceptor. *Proceedings of the National Academy of Sciences of the United States of America*, **116**, 1116–1125. https://doi.org/10.1073/pnas.0507187102

Carranco, R., Espinosa, J.M., Prieto-Dapena, P., Almoguera, C. & Jordano, J. (2010) Repression by an auxin/indole acetic acid protein connects auxin signaling with heat shock factor-mediated seed longevity. *Proceedings of the National Academy of Sciences of the United States of America*, **107**, 21908–21913. https://doi.org/10.1073/pnas.1014856107

Chaves, I., Pokorny, R., Byrdin, M., Hoang, N., Ritz, T., Brettel, K. et al. (2011) The cryptochromes: blue light photoreceptors in plants and animals. *Annual Review of Plant Biology*, **62**, 335–364. https://doi.org/10.1146/annurev-arplant-042110-103759

Chen, M. & Chory, J. (2011) Phytochrome signaling mechanisms and the control of plant development. *Trends in Cell Biology*, **21**, 664–671. https://doi.org/10.1016/j.tcb.2011.07.002

Christie, J.M. (2007) Phototropin blue-light receptors. *Annual Review of Plant Biology*, **58**, 21–45. https://doi.org/10.1146/annurev.arplant.58.032806.103951

Christie, J.M., Arvai, A.S., Baxter, K.J., Heilmann, M., Pratt, A.J., O'Hara, A. et al. (2012) Plant UVR8 photoreceptor senses UV-B by tryptophan-mediated disruption of cross-dimer salt bridges. *Science*, **335**, 1492–1496. https://doi.org/10.1126/science.1218091

Cloix, C., Kaiserli, E., Heilmann, M., Baxter, K.J., Brown, B.A., O'Hara, A. et al. (2012) C-terminal region of the UV-B photoreceptor UVR8 initiates signaling through interaction with the COP1 protein. *Proceedings of the National Academy of Sciences of the United States of America*, **109**, 16366–16370. https://doi.org/10.1073/pnas.1210898109

Deng, X.W., Caspar, T. & Quail, P.H. (1991) Cop1: a regulatory locus involved in light-controlled development and gene expression in Arabidopsis. *Genes & Development*, **5**, 1172–1182. https://doi.org/10.1101/gad.5.7.1172

Diaz-Martin, J., Almoguera, C., Prieto-Dapena, P., Espinosa, J.M. & Jordano, J. (2005) Functional interaction between two transcription factors involved in the developmental regulation of a small heat stress protein gene promoter. *Plant Physiology*, **139**, 1483–1494. https://doi.org/10.1104/pp.105.069963

Dong, H., Liu, X., Zhang, C., Guo, H., Liu, Y., Chen, H. et al. (2021) Expression of tomato UVR8 in Arabidopsis reveals conserved photoreceptor function. *Plant Science*, **303**, 110766. https://doi.org/10.1016/j.plantsci.2020.110766

Favory, J.J., Stec, A., Gruber, H., Rizzini, L., Oravecz, A., Funk, M. et al. (2009) Interaction of COP1 and UVR8 regulates UV-B-induced photomorphogenesis and stress acclimation in Arabidopsis. *The EMBO Journal*, **28**, 591–601. https://doi.org/10.1038/emboj.2009.4

Fernández, M.B., Lamattina, L. & Cassia, R. (2020) Functional analysis of the UVR8 photoreceptor from the monocotyledonous Zea mays. *Plant Growth Regulation*, **92**, 307–318. https://doi.org/10.1007/s10725-020-00639-8

Fernandez, M.B., Tossi, V., Lamattina, L. & Cassia, R. (2016) A Comprehensive phylogeny reveals functional conservation of the UV-B photoreceptor UVR8 from green algae to higher plants. *Frontiers in Plant Science*, **7**, 1698. https://doi.org/10.3389/fpls.2016.01698

Franklin, K.A. & Quail, P.H. (2010) Phytochrome functions in Arabidopsis development. *Journal of Experimental Botany*, **61**, 11–24. https://doi.org/10.1093/jxb/erp304

Gangappa, S.N. & Botto, J.F. (2016) The multifaceted roles of HY5 in plant growth and development. *Molecular Plant*, **9**, 1353–1365. https://doi.org/10.1016/j.molp.2016.07.002

Gruber, H., Heijde, M., Heller, W., Albert, A., Seidlitz, H.K. & Ulm, R. (2010) Negative feedback regulation of UV-B-induced photomorphogenesis and stress acclimation in Arabidopsis. *Proceedings of the National Academy of Sciences of the United States of America*, **107**, 20132–20137. https://doi.org/10.1073/pnas.0914532107

Guo, M., Liu, J.H., Ma, X., Luo, D.X., Gong, Z.H. & Lu, M.H. (2016) The plant Heat Stress Transcription Factors (HSFs): Structure, regulation, and function in response to abiotic stresses. *Frontiers in Plant Science*, **7**, 114. https://doi.org/10.3389/fpls.2016.00114

Heilmann, M., Christie, J.M., Kennis, J.T., Jenkins, G.I. & Mathes, T. (2015) Photoinduced transformation of UVR8 monitored by vibrational and fluorescence spectroscopy. *Photochemical & Photobiological Sciences*, **14**, 252–257. https://doi.org/10.1039/c4pp00246f

Heilmann, M., Velanis, C.N., Cloix, C., Smith, B.O., Christie, J.M. & Jenkins, G.I. (2016) Dimer/monomer status and in vivo function of salt-bridge mutants of the plant UV-B photoreceptor UVR8. *The Plant Journal*, **88**, 71–81. https://doi.org/10.1111/tpj.13260

Jiang, J., Liu, J., Sanders, D., Qian, S., Ren, W., Song, J. et al. (2021) UVR8 interacts with de novo DNA methyltransferase and suppresses DNA methylation in Arabidopsis. *Nature Plants*, **7**, 184–197. https://doi.org/10.1038/s41477-020-00843-4

Kaiserli, E. & Jenkins, G.I. (2007) UV-B promotes rapid nuclear translocation of the Arabidopsis UV-B-specific signaling component UVR8 and activates its function in the nucleus. *Plant Cell*, **19**, 2662–2673. https://doi.org/10.1105/tpc.107.053330

Kliebenstein, D.J., Lim, J.E., Landry, L.G. & Last, R.L. (2002) Arabidopsis UVR8 regulates ultraviolet-B signal transduction and tolerance and contains sequence similarity to human Regulator of Chromatin Condensation 1. *Plant Physiology*, **130**, 234–243. https://doi.org/10.1104/pp.005041

Kotak, S., Vierling, E., Baumlein, H. & Koskull-Doring, P. (2007) A novel transcriptional cascade regulating expression of heat stress proteins during seed development of Arabidopsis. *Plant Cell*, **19**, 182–195. https://doi.org/10.1105/tpc.106.048165

Lau, K., Podolec, R., Chappuis, R., Ulm, R. & Hothorn, M. (2019) Plant photoreceptors and their signaling components compete for COP1 binding via VP peptide motifs. *The EMBO Journal*, **38**, e102140. https://doi.org/10.15252/embj.2019102140

Liang, T., Mei, S., Shi, C., Yang, Y., Peng, Y., Ma, L. et al. (2018) UVR8 interacts with BES1 and BIM1 to regulate transcription and photomorphogenesis in Arabidopsis. *Developmental Cell*, **44**, 512–523.e5. https://doi.org/10.1016/j.devcel.2017.12.028

Liao, X., Zhang, B., Blatt, M.R. & Zhang, B. (2019) A FRET method for investigating dimer/monomer status and conformation of the UVR8 photoreceptor. *Photochemical & Photobiological Sciences*, **18**, 367–374. https://doi.org/10.1039/C8PP00489G

Liu, X., Zhang, Q., Yang, G., Zhang, C., Dong, H., Liu, Y. et al. (2020) Pivotal roles of Tomato photoreceptor SlUVR8 in seedling development and UV-B stress tolerance. *Biochemical and Biophysical Research Communications*, **522**, 177–183. https://doi.org/10.1016/j.bbrc.2019.11.073

Mao, K., Wang, L., Li, Y.Y. & Wu, R. (2015) Molecular cloning and functional analysis of UV RESISTANCE LOCUS 8 (PeUVR8) from Populus euphratica. *PLoS One*, **10**, e0132390. https://doi.org/10.1371/journal.pone.0132390

Miyamori, T., Nakasone, Y., Hitomi, K., Christie, J.M., Getzoff, E.D. & Terazima, M. (2015) Reaction dynamics of the UV-B photosensor UVR8. *Photochemical & Photobiological Sciences*, **14**, 995–1004. https://doi.org/10.1039/c5pp00012b

Oravecz, A., Baumann, A., Mate, Z., Brzezinska, A., Molinier, J., Oakeley, E.J. et al. (2006) CONSTITUTIVELY PHOTOMORPHOGENIC1 is required for the UV-B response in Arabidopsis. *Plant Cell*, **18**, 1975–1990. https://doi.org/10.1105/tpc.105.040097

Oyama, T., Shimura, Y. & Okada, K. (1997) The Arabidopsis HY5 gene encodes a bZIP protein that regulates stimulus-induced development of root and hypocotyl. *Genes & Development*, **11**, 2983–2995. https://doi.org/10.1101/gad.11.22.2983

Personat, J.M., Tejedor-Cano, J., Prieto-Dapena, P., Almoguera, C. & Jordano, J. (2014) Co-overexpression of two Heat Shock Factors results in enhanced seed longevity and in synergistic effects on seedling tolerance to severe dehydration and oxidative stress. *BMC Plant Biology*, **14**, 56. https://doi.org/10.1186/1471-2229-14-56

Podolec, R., Lau, K., Wagnon, T.B., Hothorn, M. & Ulm, R. (2021) A constitutively monomeric UVR8 photoreceptor confers enhanced UV-B photomorphogenesis. *Proceedings of the National Academy of Sciences of the United States of America*, **118**, e2017284118. https://doi.org/10.1073/pnas.2017284118

Prieto-Dapena, P., Almoguera, C., Personat, J.M., Merchan, F. & Jordano, J. (2017) Seed-specific transcription factor HSFA9 links late embryogenesis and early photomorphogenesis. *Journal of Experimental Botany*, **68**, 1097–1108. https://doi.org/10.1093/jxb/erx020

Prieto-Dapena, P., Castaño, R., Almoguera, C. & Jordano, J. (2006) Improved resistance to controlled deterioration in transgenic seeds. *Plant Physiology*, **142**, 1102–1112. https://doi.org/10.1104/pp.106.087817

Prieto-Dapena, P., Castaño, R., Almoguera, C. & Jordano, J. (2008) The ectopic overexpression of a seed-specific transcription factor, HaHSFA9, confers tolerance to severe dehydration in vegetative organs. *The Plant Journal*, **54**, 1004–1014. https://doi.org/10.1111/j.1365-313X.2008.03465.x

Qian, C., Chen, Z., Liu, Q., Mao, W., Chen, Y., Tian, W. et al. (2021) Coordinated transcriptional regulation by the UV-B photoreceptor and multiple transcription factors for plant UV-B responses. *Molecular Plant*, **13**, 777–792. https://doi.org/10.1016/j.molp.2020.02.015

Qian, C., Mao, W., Liu, Y., Ren, H., Lau, O.S., Ouyang, X. et al. (2016) Dual-source nuclear monomers of UV-B light receptor direct photomorphogenesis in Arabidopsis. *Molecular Plant*, **9**, 1671–1674. https://doi.org/10.1016/j.molp.2016.10.005

Rai, N., Neugart, S., Yan, Y., Wang, F., Siipola, S.M., Lindfors, A.V. et al. (2019) How do cryptochromes and UVR8 interact in natural and simulated sunlight? *Journal of Experimental Botany*, **70**, 4975–4990. https://doi.org/10.1093/jxb/erz236

Rizzini, L., Favory, J.J., Cloix, C., Faggionato, D., O'Hara, A., Kaiserli, E. et al. (2011) Perception of UV-B by the Arabidopsis UVR8 protein. *Science*, **332**, 103–106. https://doi.org/10.1126/science.1200660

Scharf, K.D., Berberich, T., Ebersberger, I. & Nover, L. (2012) The plant heat stress transcription factor (Hsf) family: structure, function and evolution. *Biochimica et Biophysica Acta*, **1819**, 104–119. https://doi.org/10.1016/j.bbagrm.2011.10.002

Song, Z., Luo, Y., Wang, W., Fan, N., Wang, D., Yang, C. et al. (2020) NtMYB12 positively regulates flavonol biosynthesis and enhances tolerance to low Pi stress in Nicotiana tabacum. *Frontiers in Plant Science*, **10**, 1683. https://doi.org/10.3389/fpls.2019.01683

Soriano, G., Cloix, C., Heilmann, M., Nunez-Olivera, E., Martinez-Abaigar, J. & Jenkins, G.I. (2018) Evolutionary conservation of structure and function of the UVR8 photoreceptor from the liverwort Marchantia polymorpha and the moss Physcomitrella patens. *The New Phytologist*, **217**, 151–162. https://doi.org/10.1111/nph.14767

Tejedor-Cano, J., Carranco, R., Personat, J.M., Prieto-Dapena, P., Almoguera, C., Espinosa, J.M. et al. (2014) A passive repression mechanism that hinders synergic transcriptional activation by heat shock factors involved in sunflower seed longevity. *Molecular Plant*, **7**, 256–259. https://doi.org/10.1093/mp/sst117

Tejedor-Cano, J., Prieto-Dapena, P., Almoguera, C., Carranco, R., Hiratsu, K., Ohme-Takagi, M. et al. (2010) Loss of function of the HSFA9 seed longevity program. *Plant, Cell & Environment*, **33**, 1408–1417. https://doi.org/10.1111/j.1365-3040.2010.02159.x

Thomas, T.T.D. & Puthur, J.T. (2017) UV radiation priming: a means of amplifying the inherent potential for abiotic stress tolerance in crop plants. *Environmental and Experimental Botany*, **138**, 57–66. https://doi.org/10.1016/j.envexpbot.2017.03.003

Tossi, V.E., Regalado, J.J., Iannicelli, J., Laino, L.E., Burrieza, H.P., Escandón, A.S. et al. (2019) Beyond Arabidopsis: differential UV-B response mediated by UVR8 in diverse species. *Frontiers in Plant Science*, **10**, 780. https://doi.org/10.3389/fpls.2019.00780

Twyffels, L., Wauquier, C., Soin, R., Decaestecker, C., Gueydan, C. & Kruys, V. (2013) A masked PY-NLS in Drosophila TIS11 and its mammalian homolog Tristetraprolin. *PLoS One*, **8**, e71686. https://doi.org/10.1371/journal.pone.0071686

Yang, Y., Liang, T., Zhang, L.B., Shao, K., Gu, X.X., Shang, R.X. et al. (2018) UVR8 interacts with WRKY36 to regulate HY5 transcription and hypocotyl elongation in Arabidopsis. *Nature Plants*, **4**, 98–107. https://doi.org/10.1038/s41477-017-0099-0

Yang, Y., Zhang, L., Chen, P., Liang, T., Li, X. & Liu, H. (2020) UV-B photoreceptor UVR8 interacts with MYB73/MYB77 to regulate auxin responses and lateral root development. *The EMBO Journal*, **39**, e101928. https://doi.org/10.15252/embj.2019101928

Yin, R., Arongaus, A.B., Binkert, M. & Ulm, R. (2015) Two distinct domains of the UVR8 photoreceptor interact with COP1 to initiate UV-B signaling in Arabidopsis. *Plant Cell*, **27**, 202–213. https://doi.org/10.1105/tpc.114.133868

Yin, R., Skvortsova, M.Y., Loubery, S. & Ulm, R. (2016) COP1 is required for UV-B-induced nuclear accumulation of the UVR8 photoreceptor. *Proceedings of the National Academy of Sciences of the United States of America*, **113**, E4415–E4422. https://doi.org/10.1073/pnas.1607074113

Yin, R. & Ulm, R. (2017) How plants cope with UV-B: from perception to response. *Current Opinion in Plant Biology*, **37**, 42–48. https://doi.org/10.1016/j.pbi.2017.03.013

Zeng, X., Ren, Z., Wu, Q., Fan, J., Peng, P.P., Tang, K. et al. (2015) Dynamic crystallography reveals early signalling events in ultraviolet photoreceptor UVR8. *Nature Plants*, **1**, 14006. https://doi.org/10.1038/nplants.2014.6

Zhao, C., Mao, K., You, C.X., Zhao, X.Y., Wang, S.H., Li, Y.Y. et al. (2016) Molecular cloning and functional analysis of a UV-B photoreceptor gene, MdUVR8 (UV Resistance Locus 8), from apple. *Plant Science*, **247**, 115–126. https://doi.org/10.1016/j.plantsci.2016.03.006